EurJIC
European Journal of Inorganic Chemistry

Full Papers
doi.org/10.1002/ejic.202100829

Chemistry Europe
European Chemical Societies Publishing

www.eurjic.org

Aminoferrocene-Based Anticancer Prodrugs Labelled with Cyanine Dyes for in vivo Imaging

Hülya Gizem Özkan,[a] Johannes Toms,[b] Simone Maschauer,[b] Olaf Prante,[b] and Andriy Mokhir*[a]

N-alkylaminoferrocene-based (NAAF) prodrugs are activated in the presence of reactive oxygen species (ROS), based on which these prodrugs target cancer cells (high ROS) and do not affect normal cells (low ROS). To gain some insights into their mode of action in vivo, we have investigated the biodistribution of ^{18}F-labelled NAAF prodrugs in tumor-bearing mice by positron emission tomography (PET). Due to the short half-life of ^{18}F, the experimental time frame was restricted to 60 min. To extend the observation window, a more stable marker is required. In this paper, we report on conjugates of NAAF prodrugs with two cyanine dyes Cy5 and Cy7 including details of their synthesis, characterization and basic properties in cell free settings and their cellular uptake in representative human cancer cells. Finally, the Cy5 conjugate was subjected to *in vivo* fluorescence imaging studies to determine the prodrug biodistribution over 24 h.

Introduction

Chemotherapy is one of the important treatment options for cancer diseases. For reduction of side effects of chemotherapeutic drugs, they can be converted to prodrugs, which are preferably activated in tumor microenvironment (TME), but remain inactive in normal cells. A number of unique for cancer cells and tumor tissue factors present in TME have been identified, which could be applied to design such prodrugs. We are especially interested in exploring reactive oxygen species (ROS) for this purpose.[1] ROS are produced in high amounts by the majority of cancer cells, whereas normal cells usually have very low amounts of ROS under homeostasis.[2] In particular, our research group has developed N-alkylaminoferrocene (NAAF) based prodrugs, which are activated by ROS with formation of NAAF drugs.[3] The latter drugs are electron rich species. They donate electrons to endogenous substrates like H_2O_2 and O_2 thereby generating highly toxic reactive species $HO^{\bullet}$ and $O_2^{\bullet-}$ correspondingly, which induce cancer cell death via necrosis and apoptosis. The mechanism of action of NAAF prodrugs in human cancer cell lines and primary human cancer cells has been thoroughly investigated.[1,3,4] However, less is known about how NAAF prodrugs elicit their antitumor effect in vivo. To address this issue, we converted representative NAAF prodrug **1** to its radioactive analogue **2**, which can be monitored in vivo by using PET. This compound was prepared by conjugation of 6-deoxy-6-[^{18}F]fluoro-β-glucopyranosyl azide[6] via the reaction of copper(I)-catalyzed azide–alkyne 1,3-dipolar cycloaddition (CuAAC).[5] The studies of the biodistribution of conjugate **2** in mice using PET provided first valuable insights into stability and tumor uptake of NAAF prodrugs in vivo.[5,7] However, their important limitation was the relatively short observation time. The reason for this limitation is the short half-life of ^{18}F (110 min), preventing prolonged imaging studies after tracer injection for more than several hours.[5,7] One possible solution of this problem could be replacing the ^{18}F-labelled glycosyl moiety with a fluorescent dye absorbing and emitting light above 600 nm. The dye of the latter type can be detected directly in live animals using commercially available small animal fluorescence imaging systems, e.g. IVIS® Spectrum In Vivo Imaging System (Perkin Elmer, Germany). Previously, we have prepared NAAF prodrugs labelled with different fluorescent dyes including coumarins,[3a,c] fluorescein[3b] and N,N,N′,N′-tetramethylrhodamine (TMR).[8] However, none of these conjugates was compatible with in vivo fluorescence imaging due to the unfavorable photophysical properties of the corresponding dyes with excitation and emission wavelengths of <550 nm.

In this paper, we present the synthesis of NAAF-prodrugs labelled with cyanine dyes Cy5 ($\lambda_{ex}=644$ nm, $\lambda_{em}=658$ nm) and Cy7 ($\lambda_{ex}=751$ nm, $\lambda_{em}=775$ nm) and their characterization both in vitro and in vivo. We selected these dyes, as they are both bright (extinction coefficient×fluorescence quantum yield) and absorb and emit light in the so-called biological window between 650 and 900 nm, where endogenous light absorbers are not active.

[a] H. Gizem Özkan, Prof. Dr. A. Mokhir
Friedrich-Alexander University Erlangen-Nürnberg (FAU)
Department of Chemistry and Pharmacy, Organic Chemistry Chair II
Nikolaus-Fiebiger-Str. 10, 91058 Erlangen, Germany
E-mail: Andriy.Mokhir@fau.de
https://www.chemie.nat.fau.de/ak-mokhir/
[b] Dr. J. Toms, Dr. S. Maschauer, Prof. Dr. O. Prante
Friedrich-Alexander University Erlangen-Nürnberg (FAU)
Department of Nuclear Medicine, Molecular Imaging and Radiochemistry
Schwabachanlage 12, 91054 Erlangen, Germany

Supporting information for this article is available on the WWW under https://doi.org/10.1002/ejic.202100829

Part of the "Ferrocene Chemistry" Special Collection.

Results and Discussion

Design and Synthesis

Our goal was to prepare labelled NAAF prodrugs, which are fluorescent both in their intact form and after the activation with formation of NAAF and NAAF$^+$ drugs. Previously, we have observed that fluorescence of the related NAAF prodrug ~ dye conjugates can be efficiently quenched due to photoinduced electron transfer (PE[9]) from the ferrocenyl moiety.[3] Since the PE effect is strongly dependent from the distance between an emitter and an electron donor, we designed NAAF prodrug ~ CyN conjugates (where N = 5, 7) in such a way that the prodrug part was separated from the CyN part by a long flexible linker consisting of over 14 atoms (Figure 1B). Conjugates **5_CyN** were prepared by coupling of a terminal alkyne in previously reported NAAF prodrug **4a**[4] to an azido group in commercially available CyN–NH$(CH_2)_3N_3$ reagents in the presence of Cu^+, which was generated *in situ* from Cu and $CuSO_4$ at 55 °C. The reaction was monitored by reverse phase thin layer chromatography (RP-TLC) and stopped (at approximately 16 h) after full conversion of the starting materials was achieved. The similar procedure was used to prepare control conjugates **6_CyN**, where a $B(OH)_2$ residue was replaced by fluorine, by using **4a** as starting material. The identity and purity of the conjugates were confirmed by ^{1}H NMR, high resolution ESI mass spectrometry and RP-TLC (experimental part of the paper and *SI*). In particular, a terminal alkyne signal "a" in ^{1}H NMR spectrum of **4a** disappears after its coupling to Cy5-NH$(CH2)_3N_3$ with formation of **5_Cy5** (Figure 2A), whereas a new signal "b" of a hydrogen atom of 1,2,3-triazolyl fragment appears (Figure 2B). Similar changes in ^{1}H NMR spectra were also observed for other prepared conjugates **5_Cy7**, **6_Cy5**, and **6_Cy7** (Figures S7, S9, S11, supporting information: *SI*). Unfortunately, Cy7 conjugates could not be obtained in > 95 % purity, due to their intrinsic instability (Figure 3), whereas Cy5 conjugates could be prepared in sufficient purity.

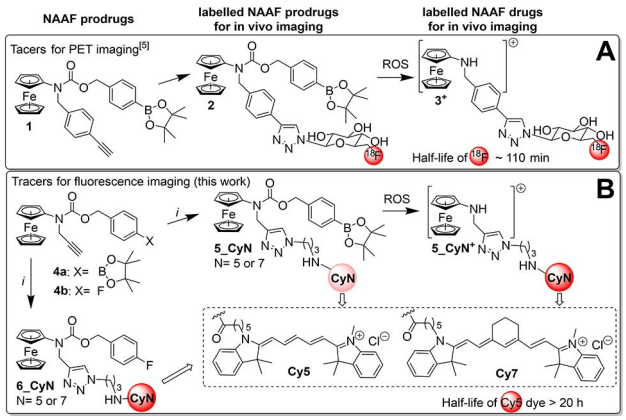

Figure 1. A: Labelling of representative NAAF prodrug **1** with ^{18}F to obtain conjugate **2**.[5] In the presence of ROS **2** is converted to NAAF **3**, which under oxidative conditions in cancer cells is further oxidized forming **3**$^+$. Conjugate **2** has been used to monitor the biodistribution of NAAF prodrugs in mice by PET for up to 60 min. A longer observation time was unfavorable due to the short half-life of the ^{18}F tracer. **B**: Labelling prodrug **4** with fluorescent dyes Cy5 or Cy7 to obtain the candidate conjugates **5_CyN** for in vivo fluorescence imaging studies. Conditions of synthetic step *i*: CyN$(CH_2)_3N_3$, (N = 5 or 7), Cu, $CuSO_4$, N,N-dimethylformamide (DMF), 55 °C. Compounds **6_CyN** are ROS-insensitive analogues of **5_CyN** and were used for comparative experiments as controls. A full mechanism of the reaction of **5_Cy5** with H_2O_2 is provided in Figure S13, *SI*.

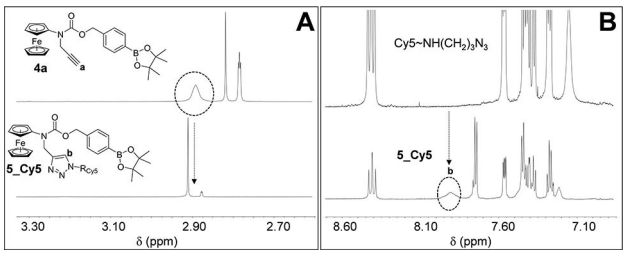

Figure 2. A: ^{1}H NMR spectra of a precursor (NAAF prodrug **4**, upper trace) and a product (Cy5-labelled NAAF prodrug **5_Cy4**, lower trace) indicating the absence of a characteristic terminal alkyne signal "a" in the spectrum of the product **5_Cy5. B**: ^{1}H NMR spectra of a precursor (Cy5 ~ NH$(CH_2)_3N_3$, the structure of Cy5 is given in Figure 1, upper trace) and a product (**5_Cy4**, lower trace) indicating the presence of a characteristic 1,2,3-tetrazol signal "b" in the spectrum of the product **5_Cy5**.

Fluorescence of the conjugates in the presence of ROS

We studied changes of fluorescence of aqueous buffered at pH 7.4 solution of conjugate **6_Cy5** (0.9 μM) in the presence of H_2O_2 (18 mM) (Figure 3A). This compound is defined as a negative control, as it contains the ROS-insensitive group (4-fluorophenyl)methyloxycarbonyl. We observed practically no change of the fluorescence intensity within 40 min (Figure 3A). In the absence of H_2O_2 the same trend was observed (data not shown). These data indicate that **6_Cy5** is stable under the conditions tested, as expected for the negative control. In contrast, fluorescence intensity of the aqueous solution of conjugate **5_Cy5** (0.9 μM) containing a ROS responsive group based on phenylboronic acid pinacol ester is significantly increased in the presence of H_2O_2 (18 mM) (Figure 3A, Figure S14, *SI*), which is in agreement with its activation according

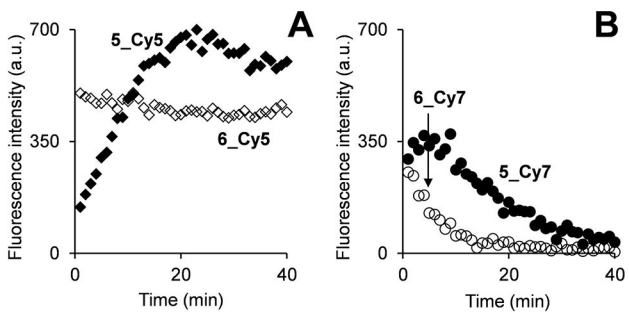

Figure 3. A: Monitoring fluorescence intensity (λ_{ex} = 644 nm, λ_{em} = 658 nm) of Cy5 conjugates (0.9 μM, indicated on the plot, structures are given in Figure 1) dissolved in phosphate buffer (7 mM, pH 7.4) containing NaCl (98 mM), KCl (1.9 mM), dimethylsulfoxide (DMSO, 0.9 %, v/v), CH_3CN (9 %, v/v) and H_2O_2 (18 mM). **B**: Monitoring fluorescence intensity (λ_{ex} = 751 nm, λ_{em} = 775 nm) of Cy7 conjugates (0.9 μM, indicated on the plot) dissolved in the same buffer as the Cy5 conjugates (see inset **A**).

to the mechanism outlined in Figure 1B and Figure S13, *SI*. In particular, in the conjugate the fluorescence of Cy5 is partially quenched due to PE from the ferrocenyl fragment. H_2O_2-induced cleavage of a B–C bond in **5_Cy5** leads in few following steps (Figure S13, *SI*) to a stronger fluorescent derivative **5_Cy5**$^+$, where the ferrocenyl fragment is oxidized and, therefore, is not capable to support PE. Similar behavior was observed previously for coumarin,[3a],[3b] fluorescein[3b] and TMR-containing NAAF prodrugs[7] indicating that **5_Cy5** behaves like a typical fluorogenic NAAF prodrug. Interestingly, **6_Cy5** exhibits the higher fluorescence than **5_Cy5** (Figure 3A, at time point 0). This might suggest that average distance between the Cy5 dye and ferrocene (acting as a quencher) is different in these compounds that would lead to different quenching efficacies.

We observed that, in contrast to the Cy5-containing NAAF prodrugs, the fluorescence of both **5_Cy7** and **6_Cy7** is decreased both in the presence of H_2O_2 (Figure 3B) and in its absence. These data indicate that the Cy7 derivatives are not stable under the conditions used and, therefore, they are not suitable as fluorogenic NAAF prodrugs. Further evaluation experiments were concerned with the stable Cy5 derivatives only.

Uptake and distribution of the Cy5 conjugates in live cells

Next, we studied uptake and distribution of labelled NAAF prodrug **5_Cy5** in representative human cancer cells A2780 (ovarian cancer). These cells were selected, since they are known to contain high levels of intracellular ROS sufficient for activation of NAAF prodrugs.[3] Previously, we observed that NAAF prodrugs without any special carriers are accumulated in mitochondria of cells after their activation with formation of ferrocenium NAAF$^+$ species (Figure 1).[3b] We investigated whether this property is retained for **5_Cy5** by using fluorescence microscopy in combination with the mitochondria-specific dye rhodamine 123 (R123). The latter dye (1 mg/L) and **5_Cy5** (100 nM) were co-incubated with A2780 cells and their co-localization was studied by using channel 1 for detection of Cy5 (Ch1: excitation λ_{ex} = 538–563 nm, emission λ_{em} = 570–640 nm) and channel 2 for detection of R123 (Ch2: λ_{ex} = 450–490 nm, λ_{em} = 500–550 nm). We carefully confirmed that the emission signal of Cy5 does not leak to the Ch2 channel and that of R123 does not leak to the Ch1 channel (Figure S15, *SI*), thereby confirming that Cy5 and R123 can be detected independently of each other under the selected experimental conditions.

The results of the co-localization experiments in A2780 cells are shown in Figure S16, *SI*. The data indicate that **5_Cy5** is efficiently taken up by A2780 cells (intense red spots in image A). When both compounds (Cy5 – red, R123 - green) co-localize in cells, the merged yellow signal is expected to appear in the combined image Ch1 + Ch2 + Ch3 (Ch3 is a bright field image). Indeed, a high degree of merged yellow signal is observed (Figure S16D, *SI*), indicating that **5_Cy5** and/or its drug product formed in cells **5_Cy5**$^+$ (Figure 1B) co-localize with R123. These data confirm that the labeled NAAF prodrug and its products are localized in mitochondria analogously to the parent, unlabeled derivatives.[3b]

This effect is not restricted to one cell line. In particular, we observed the same behavior of **5_Cy5** in human prostate cancer DU-145 cells (Figure 4).

Interestingly, the ROS-insensitive analogue **6_Cy5** also intracellularly accumulated in both A2780 and DU-145 cells. Furthermore, **6_Cy5** is localized in mitochondria of the cancer cells similarly to ROS-sensitive **5_Cy5** (Figure S16, *SI* and Figure 4). These data might indicate that the uptake and distribution of Cy5-derivatives with NAAF prodrugs and ROS-insensitive controls is defined by the Cy5 dye rather than by the NAAF-part of the molecule.

Next, we investigated the uptake of **5_Cy5** by representative non-malignant cells, applying normal human dermal fibroblasts (NHDF) (Figure 5). In contrast to the cancer cells A2780 and DU-145, we did not detect any cellular fluorescence signal (red channel Ch1) after incubation of **5_Cy5** (100 nM)

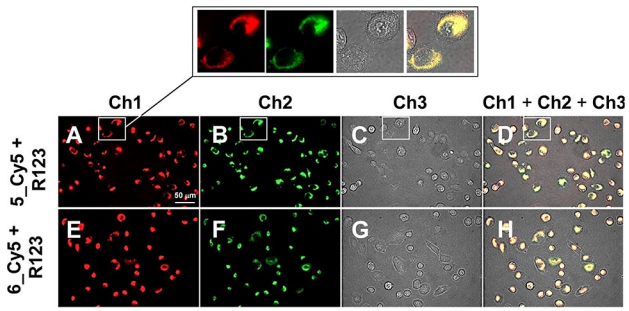

Figure 4. Images of DU145 cells. Ch1: excitation λ_{ex} = 538–563 nm, emission λ_{em} = 570–640 nm), Ch2: λ_{ex} = 450–490 nm, λ_{em} = 500–550 nm, Ch3: bright-field images. **A**-**D**: Data for the cells incubated with a mixture of **5_Cy5** (100 nM) and R123 (1 mg/L) for 20 min. **E**-**H**: Data for the cells incubated with a mixture of **6_Cy5** (100 nM) and R123 (1 mg/L) for 20 min. A zoom in area (labelled with a white box) is shown separately.

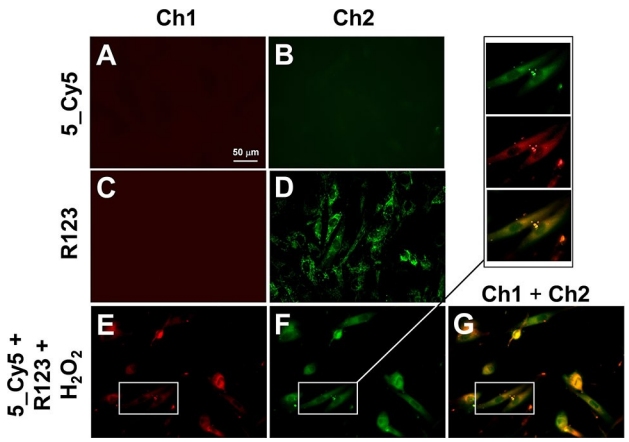

Figure 5. Images of NHDF cells. Ch1 and Ch2 are defined in caption to Figure 4. **A**, **B**: Data for the cells incubated with **5_Cy5** (100 nM) for 20 min. **C**, **D**: Data for the cells incubated with R123 (1 mg/L) for 20 min. **E**-**G**: Data for the cells incubated with a mixture of **5_Cy5** (100 nM), R123 (1 mg/L) for 20 min, washed and further incubated with H_2O_2 (10 mM) for 10 min.

with NHDF. Two possible explanations of this observation are: (a) weak or no detectable cellular uptake of **5_Cy5** prodrug or (b) the absence of ROS-induced activation of **5_Cy5** in NHDF with formation of highly fluorescent product **5_Cy5**$^+$ (Figure 2, Figure S13, *SI*). Normal cells often accumulate chemical compounds less efficiently than cancer cells, due to their low metabolism. However, we observed that NHDF are capable to accumulate other dyes as efficiently as cancer cells: see, e.g., the data for R123 shown in Figure 5D for NHDF and in Figure S16F, *SI* for A2780 cells, 4B, F for DU-145 cells. Interestingly, we observed that treatment with H_2O_2 (10 mM) of NHDF that were pre-incubated with **5_Cy5** (100 nM) leads to an increased appearance of intense red fluorescence in Ch1 channel. These data indicate that **5_Cy5** is taken up by NHDF to some degree, but is not activated with formation of fluorescent **5_Cy5**$^+$ due to the absence of sufficient amounts of ROS in normal cells.

Distribution of 5_Cy5 in vivo

Based on the above discussed data, fluorogenic **5_Cy5** behaves like a typical NAAF prodrug. In particular, it is activated in cancer cells and the resulting product drug is accumulated in mitochondria. The activation of this type does not occur in normal cells lacking elevated ROS levels. Furthermore, the product generated from **5_Cy5** in cells is highly fluorescent in the red spectral area, which is highly favorable for its detection *in vivo*.

Encouraged by these favorable results from the in vitro experiments, we studied the biodistribution of **5_Cy5** in vivo and compared it to that of free dye **Cy5**-OH. The latter was used to reveal the role of the NAAF part in biodistribution of **5_Cy5**. We applied mice bearing simultaneously two xenografts (human prostate tumor PC-3, right shoulder (view from the top) and rat pancreatic tumor AR42J, left shoulder, n = 7) and injected either **5_Cy5** (2 nmol/mouse, n = 4) or the dye **Cy5**-OH (2 nmol/mouse, n = 3) in aqueous NaCl (0.9%, m/v) containing DMSO (1%, v/v) (100 μL). The mode of injection was either intravenous (i.v., n = 4: 2× for **5_Cy5** and 2× for the control) or subcutaneous (s.c., n = 3: 2× for 5_Cy5 and 1× for the control). During the imaging experiments, no signs of acute toxicity were observed when using the indicated injection dose. Longitudinal imaging of animals using the in vivo imaging system IVIS at 1–24 h postinjection (p.i.) of **5_Cy5** for monitoring changes of tumor uptake turned out to be inadequate due to the low signal-to-noise ratio. Therefore, the mice were euthanized at 24 h p.i. under anesthesia and selected organs and tumors were dissected for *ex vivo* analysis of their fluorescence by using the IVIS scanner (Figure 6, Figure 7).

The highest accumulation was detected in the stomach, the intestine and kidneys. **5_Cy5** and **Cy5**-OH exhibited a similar biodistribution, indicating that the dye Cy5 affects strongly the *in vivo* biodistribution of both conjugates (Figure 6). In the presence of strong signals (stomach, other organs), weaker signals (tumors) are detected inaccurately. Therefore, we analyzed both tumors of each mouse separately (Figure 7). In

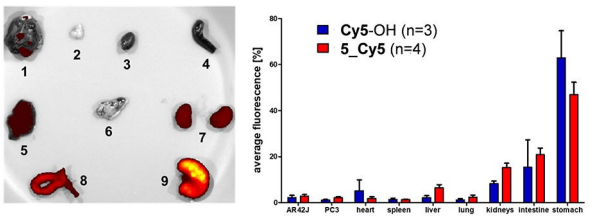

Figure 6. *Ex-vivo* (24 h p.i.) optical imaging of organs (left side) of tumor-bearing mice (AR42J and PC-3) injected intravenously or subcutaneously with **5_Cy5** or **Cy5**-OH and corresponding fluorescence-dependent biodistribution (right side). Numbers in left images represent the removed organs: 1) AR42J tumor 2) PC-3 tumor 3) heart 4) spleen 5) liver 6) lung 7) kidneys 8) part of intestine 9) stomach.

AR42J tumors, the uptake of **5_Cy5** was highly heterogenous and the difference of tumor fluorescence between **5_Cy5**- and **Cy5-OH**-injected animals was not statistically significant ($P = 0.33$, unpaired t-test, Figure 7, left). However, interestingly **5_Cy5** revealed significantly higher uptake in PC-3 tumors compared to **Cy5**-OH ($P < 0.05$, unpaired t-test, Figure 7, right), suggesting specific and ROS-dependent tumor uptake of **5_Cy5**.

Conclusion

We successfully prepared a representative N-alkylaminoferrocene-based prodrug labelled with a cyanine 5 dye (**5_Cy5**), which absorbs and emits light at wavelengths >600 nm. Previously known fluorogenic prodrugs of this type were absorbing and emitting light <550 nm and, therefore, were not suitable for *in vivo* imaging. We demonstrated that **5_Cy5** is activated in cell free settings in the presence of ROS with formation of a fluorescent product **5_Cy5**$^+$. Furthermore, we found that **5_Cy5** is efficiently taken up by two studied cancer cells (A2780 and DU-145) and products released in cells are accumulated in their mitochondria. As expected, **5_Cy5** demonstrated uptake in representative normal cells (NHDF) to some degree, but its conversion to **5_Cy5**$^+$ does not occur due to the low level of ROS in normal cells. Finally, we monitored the biodistribution of **5_Cy5** *in vivo* in mice carrying human prostate and rat pancreatic tumors over 24 h. As compared to negative control **Cy5**-OH, we observed that accumulation of prodrug **5_Cy5** in PC-3 tumors is higher than that of **Cy5**-OH. Overall, the accumulation in tumors was not high that is in agreement with the data obtained previously with ^{18}F-labelled NAAF prodrugs in tumor-bearing mice by using positron emission tomography (PET).[5] One possible explanation of that is unspecific oxidation of NAAF prodrugs in the point of injection and in healthy tissues including stomach, intestine, kidneys and liver (Figure 6).

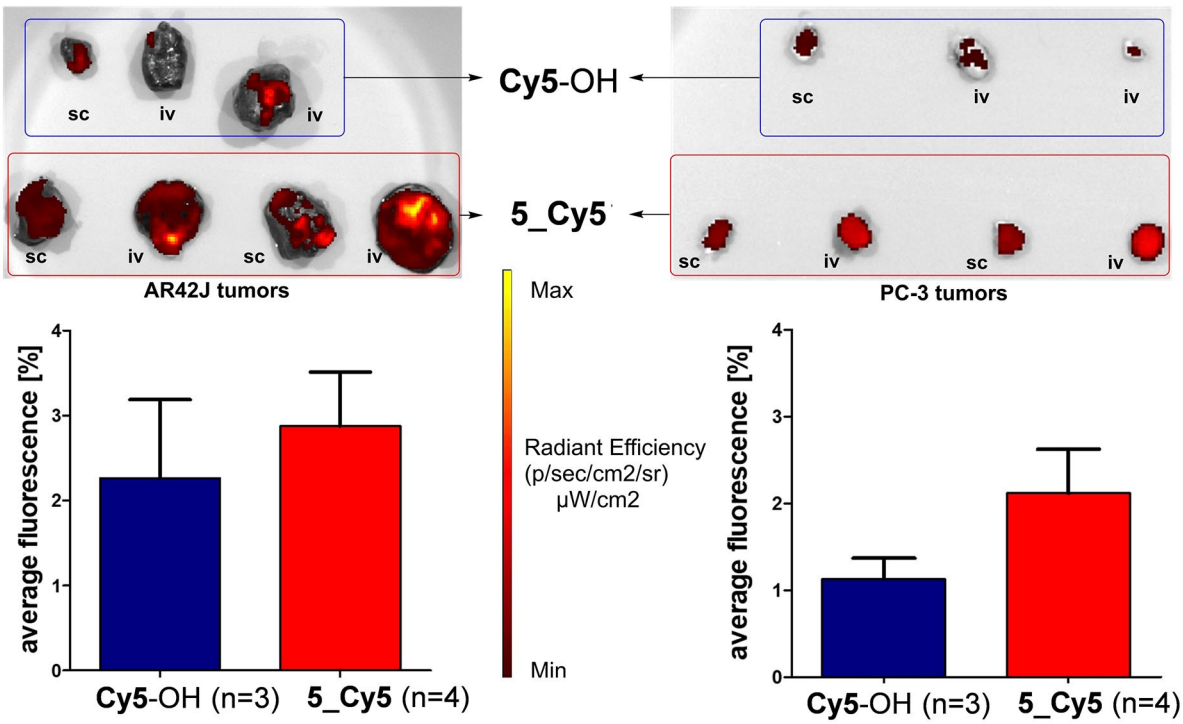

Figure 7. Optical imaging of all tumors after dissection of mice injected either with **5_Cy5** prodrug or with **Cy5**-OH intravenously (iv) or subcutaneously (sc) at 24 h postinjection. Below the red bars represent the average fluorescence measured for tumors (left: AR42J; right: PC-3) treated with **5_Cy5** prodrug. The blue bars represent the average fluorescence measured for tumors of mice treated with **Cy5**-OH for comparison.

Experimental Section

Commercially available chemicals of the best quality from Merck (Taufkirchen), Alfa-Aesar (Kandel) and Lumiprobe (Hannover) were obtained and used without purification. NMR spectra were acquired on a Bruker Avance 400 or Bruker Avance 600 (Ettlingen, Germany). Electrospray ionization (ESI) mass spectra were recorded on a Bruker ESI MicroTOF II (Bremen, Germany) or Bruker maXis 4G mass spectrometers (Bremen, Germany). Fluorescence spectra were acquired on Cary Eclipse fluorescence spectrophotometer (Agilent, Waldbronn) by using quartz glass cuvettes with a sample volume of 1 mL. The fluorescence images of live cells were acquired by using an Axio Vert.A1 microscope (Zeiss, Oberkochen) using 40x/1.30 objective (oil DIC).

Synthesis

Conjugate **5_Cy5**. Cy5-NH$(CH_2)_3N_3$ (Cyanin-5-azid (Lumiprobe), 3.75 mg, 6.24 μmol) was dissolved in anhydrous DMF (50 μL) under argon atmosphere. Compound **4a** (3.1 mg, 6.21 μmol), Cu (3.2 mg, 50.35 μmol) and water free $CuSO_4$ (1.25 mg, 7.83 μmol) were combined in another glass vial. These compounds were suspended in DMF (2×30 μL) and the suspension was added to the solution of Cy5-NH$(CH_2)_3N_3$. The mixture was flashed with Ar (3 min), sealed with parafilm and covered with aluminium foil to protect it from day light. The reaction mixture was shaken at 1100 rpm at 55 °C for 4 h and at 25 °C for additional 16 h. Subsequently, the mixture was centrifuged (13400 rpm, 1 min) and the supernatant was split as 5× 20 μL portions. The remaining copper residue was washed three times with DMF (3×20 μL) and combined in another portion. The crude product in each portion was precipitated with the slow addition of water (1.5 mL) and the resulting mixtures were centrifuged (13400 rpm, 15 min, 3×). The water was removed, and the products were combined by dissolving them in acetone. The solvent was removed, and the product was obtained as blue solid (5.52 mg, 5.04 μmol, 81 %). RP-TLC (eluent: CH_3CN/phosphate saline buffer (pH 7.4); 8.5/1.5; v/v) R_f = 0.47 (R_f of Cy5-NH$(CH_2)_3N_3$ = 0.52). ^{1}H-NMR: (601 MHz, Acetone-d6) δ 8.40 (dd, J = 13.8, 12.4 Hz, 2H), 7.90 (s, 1H), 7.76–7.73 (m, 2H), 7.57–7.53 (m, 2H), 7.45–7.35 (m, 6H), 7.26 (qd, J = 7.5, 1.2 Hz, 2H), 7.21 (s, 1H), 6.64 (s, 1H), 6.43 (d, J = 13.7 Hz, 1H), 6.34 (d, J = 13.7 Hz, 1H), 5.23 (s, 2H), 4.99 (s, 2H), 4.39 (s, 2H), 4.23–4.12 (m, 4H), 4.09 (s, 5H), 3.97 (t, J = 2.0 Hz, 2H), 3.68 (s, 3H), 3.20 (d, J = 7.4 Hz, 2H), 1.85–1.82 (m, 2H), 1.70 (s, 12H), 1.59–1.53 (m, 2H), 1.51–1.47 (m, 2H), 1.31 (s, 12H), 1.27 (s, 4H). ^{13}C NMR (151 MHz, Acetone) δ 206.24, 174.59, 173.96, 172.98, 154.95, 145.58, 143.94, 143.16, 142.12, 142.03, 135.62, 130.50, 130.49, 129.44, 129.37, 128.15, 126.15, 125.81, 123.15, 123.03, 111.92, 111.72, 104.12, 104.07, 84.56, 69.63, 69.31, 69.27, 67.85, 65.05, 50.05, 49.98, 48.23, 44.56, 36.72, 36.20, 29.84, 27.82, 27.72, 27.57, 26.96, 26.96, 26.26, 25.81, 25.16, 23.30. HR-MS (ESI+), *m/z* calculated for $C_{62}H_{75}BFeN_7O_5$ 1064.5272, found 1064.5272.

Conjugate **5_Cy7**. This compound was prepared analogously to **5_Cy5**, except that Cy7-NH$(CH_2)_3N_3$ (Cyanin-7-azid (Lumiprobe), 4.12 mg, 6.17 μM) was used in place of Cyanin-5-azid. The conjugate was obtained as a blue solid. Yield: 5.9 mg, 5.06 μmol, 70 %. RP-TLC (eluent: CH_3CN/phosphate saline buffer (pH 7.4); 8.5/1.5; v/v) R_f = 0,40. ^{1}H-NMR: (601 MHz, Acetone-d6) δ 7.88 (s, 1H), 7.79 (dd, J = 14.1, 7.7 Hz, 2H), 7.74 (t, J = 7.4 Hz, 2H), 7.60 (s, 1H), 7.54 (t, J = 6.7 Hz, 2H), 7.46–7.31 (m, 7H), 7.26–7.22 (m, 2H), 6.29 (d, J = 14.1 Hz, 1H), 6.25 (d, J = 14.1 Hz, 1H), 5.23 (s, 2H), 4.99 (s, 2H), 4.38 (s, 2H), 4.24–4.15 (m, 4H), 4.09 (s, 5H), 3.97 (t, J = 2.0 Hz, 2H), 3.70 (s, 3H), 3.54–3.50 (m, 2H), 2.59–2.51 (m, 4H), 1.87–1.84 (m, 2H), 1.72 (s, 12H), 1.59–1.53 (m, 4H), 1.51–1.47 (m, 2H), 1.31 (s, 12H) 1.27(overlapping, 4H). HR-MS (ESI+) *m/z* calculated for $C_{67}H_{81}BFeN_7O_5$ 1130.5749, found 1130.5745.

Conjugate **6_Cy5**. Cy5-NH$(CH_2)_3N_3$ (Cyanin-5-azid (Lumiprobe), 5.38 mg, 8.95 μmol) was dissolved in anhydrous DMF (50 μL) under argon atmosphere. Compound **4b** (3.5 mg, 8.95 μmol), Cu (4.55 mg, 71.57 μmol) and water free $CuSO_4$ (1.78 mg, 11.18 μmol) were combined in another glass vial. DMF (12 μL) was added and the resulting suspension was transferred to the solution of Cy5-NH$(CH_2)_3N_3$. The mixture was flashed with Ar (3 min), sealed with parafilm and covered with aluminum foil. The reaction mixture was shaken at 1100 rpm at 55 °C for 4 h and at 25 °C for additional 16 h. Subsequently, the mixture was centrifuged (13400 rpm, 15 min) and the supernatant was split as 4×15 μL portions. The remaining copper residue was washed three times with DMF (3×15 μL) and obtained solutions were combined in another portion. The crude product in each portion was precipitated with the slow addition of water (1.5 mL) and the resulting mixtures were centrifuged (13400 rpm, 15 min, 3×). The water was removed, and the products were combined by dissolving them in acetone. The solvent was removed, and the product was obtained as blue solid (5.33 mg, 5.37 μmol, 60%). RP-TLC (eluent: CH_3CN/phosphate saline buffer (pH 7.4); 8.5/1.5; v/v) $R_f = 0.46$ (R_f of Cy5-NH$(CH_2)_3N_3 = 0.52$). ^{1}H-NMR: (601 MHz, Acetone-d6) δ 8.40 (dd, J = 13.2 Hz, 2H), 7.89 (s, 1H), 7.62–7.53 (m, 2H), 7.53–6.99 (m, 10H), 7.22–7.16 (s, 1H), 6.67 (t, J = 12.4 Hz, 1H), 6.44 (d, J = 13.7 Hz, 1H), 6.36 (d, J = 13.8 Hz, 1H), 5.21 (s, 2H), 4.98 (s, 2H), 4.64 (s, 2H), 4.41 (m, 4H), 4.08 (s, 5H), 3.97 (t, J = 1.8 Hz, 2H), 3.70 (s, 3H), 3.22 (d, J = 6.4 Hz, 2H), 1.91 (m, 2H), 1.72 (s, 12H), 1.29 (s, 8H). ^{13}C NMR (151 MHz, Acetone) δ 206.13, 174.74, 174.15, 173.82, 173.10, 172.79, 164.22, 162.60, 155.04, 154.93, 145.64, 144.01, 143.25, 142.24, 142.10, 133.95, 131.43, 131.38, 130.58, 130.56, 129.50, 129.43, 126.25, 125.89, 124.18, 123.20, 123.08, 116.15, 116.01, 112.00, 111.77, 104.18, 70.88, 69.67, 67.32, 66.18, 65.09, 64.07, 50.14, 50.06, 49.79, 48.37, 44.68, 37.09, 36.86, 36.29, 36.12, 34.55, 32.64, 29.84, 27.85, 27.84, 27.82, 27.80, 27.78, 27.67, 27.04, 25.87, 25.67, 23.33, 14.35. HR-MS (ESI+) *m/z* calculated for $C_{56}H_{63}FFeN_7O_3$ 956.4322, found 956.4315.

Conjugate **6_Cy7**. This compound was prepared analogously to **6_Cy5**, except that Cy7-NH$(CH_2)_3N_3$ (Cyanin-7-azid (Lumiprobe), 5.97 mg, 8.95 μM) was used in place of Cyanin-5-azid. The conjugate was obtained as a blue solid. Yield: 6.96 mg, 6.57 μmol, 74%. RP-TLC (eluent: CH_3CN/phosphate saline buffer (pH 7.4); 8.5/1.5; v/v) $R_f = 0.40$ (R_f Cy7-NH$(CH_2)_3N_3 = 0.44$). HR-MS (ESI+) *m/z* calculated for $C_{61}H_{69}FFeN_7O_3$, 1022,4791 found 1022,4776.

Monitoring fluorescence of the conjugates in the presence of H_2O_2

The conjugates were dissolved in DMSO (100 μM). This solution (10 μL) was diluted with phosphate saline buffer (PBS, pH 7.4, phosphate 10 mM, NaCl 137 mM, KCl 2.7 mM, volume 790 μL), acetonitrile (100 μL) and water (100 μL). Next, H_2O_2 (200 mM, 100 μL) was added (final concentration 18 mM) and the fluorescence monitoring started. Cy5 conjugates at 644 nm and the fluorescence were recorded at 658 nm over 40 min. Cy7 conjugates were excited at 751 nm and the fluorescence was recorded at 775 nm over 40 min.

Experiments with cells

Human ovarian cancer cell line (A2780) was obtained from Sigma-Aldrich. Cells were grown in RPMI 1640 medium supplemented with 10% FBS (Sigma-Aldrich), 1% L-glutamine, and 1% penicillin/streptomycin. The human prostate carcinoma cell line DU145 was purchased from CLS Cell Lines Service GmbH (Eppelheim, Germany). Normal human dermal fibroblasts cell line (NHDF) was a kind gift of Dr. Christina Janko (Clinic of Otolaryngology, Friedrich-Alexander-University Hospital Erlangen). DU145 and NHDF cell lines were grown in Dulbecco's Minimal Essential Medium (DMEM) with phenol red as indicator, supplemented with 10% FBS, 1% of L-glutamine and 1% of penicillin/streptomycin. All adherent cells were cultivated to 80 − 90% confluence and detached from the flask by using trypsin/N,N,N′,N′-ethylenediamine tetraacetic acid (EDTA) solution (0.025%/0.01%, w/v) in PBS.

Localization of **5_Cy5**, **6_Cy5** and R123 in cancer cell by using fluorescence microscopy. A2780 cells (in 2 mL RPMI 1640 medium containing 5% FBS, 1% L-glutamine and 1% penicillin/streptomycin) and DU-145 (in 2 mL DMEM without phenol red containing 5% FBS, 1% L-glutamine and 1% penicillin/streptomycin) were seeded on a 35 mm imaging dish (μ-Dish 35 mm, high, ibidi GmbH, Germany) at a cell density of 80 cells/μL one day before the experiment in RPMI 1640 medium (2 mL) containing 5% FBS, 1% L-glutamine and 1% penicillin/streptomycin. On the next day, the cells were washed with DPBS (2×2 mL). A fresh portion of RPMI 1640 medium (2 mL) was added. Conjugate **5_Cy5** (or **6_Cy5**) in DMSO (stock solution 10 μM, final concentration 100 nM) or R123 in DMSO (stock solution 100 mg/L, final concentration 1 mg/L) were added and incubated in the incubator at 37 °C containing 5% CO_2 for 20 min. The cells were washed with DPBS (2×2 mL) and the fresh medium (2 mL) was added. The fluorescence images were taken with a Zeiss Axio Vert.A1 and filter set: excitation/emission 538–563/570–640 nm for the detection of Cy5 and 450–490/500–550 nm for the detection of R123. Objective: 40x/1.30. Oil DIC.

Co-localization experiments were conducted similarly, except that mixtures of the conjugates and R123 were added.

Monitoring activation of **5_Cy5** in NHDF with H_2O_2. NHDF cells were seeded on a 35 mm imaging dish (μ-Dish 35 mm, high, ibidi GmbH, Germany) at a cell density of 40 cells/μL one day before the experiment in DMEM (2 mL) containing 5% FBS, 1% L-glutamine and 1% penicillin/streptomycin. On the next day, the cells were washed with DPBS (2×2 mL). A fresh portion of DMEM (2 mL) was added. Conjugate **5_Cy5** in DMSO (stock solution 20 μM, final concentration 100 nM) and R123 in DMSO (stock solution 200 mg/L, final concentration 1 mg/L) were added and incubated at 37 °C containing 5% CO_2 for 20 min. The cells were washed with DPBS (2×2 mL) and H_2O_2 (10 mM) was added. The cells were incubated for 10 min, then washed, and fresh medium (2 mL) was added. The fluorescence images were taken with a Zeiss Axio Vert.A1 and filter set: excitation/emission 538–563/570–640 nm for the detection of Cy5 and 450–490/500–550 nm for the detection of R123. Objective: 40x/1.30. Oil DIC.

In vivo fluorescence imaging and biodistribution studies

All animal experiments were performed in compliance with the protocols approved by the local Animal Protection Authorities (Regierung Mittelfranken, Germany, no. 54-2532.1-15/08) and performed at the FAU in accordance with the relevant E.U. guidelines and regulations. Female athymic nude mice (CD1-Foxn1/nu, homozygous) were obtained from Charles River Laboratories (Sulzfeld, Germany) at 4 weeks of age and were kept under standard conditions (12 h light/dark) with food and water available ad libitum for at least 5 weeks. Viable tumor cells were harvested, suspended in PBS/Matrigel (1:1, 100 μL) and were injected subcutaneously in the left (2×10^6 PC-3 cells/mouse) and right (2.5×10^6 AR42J cells/mouse) side of the back of each mouse under isoflurane anesthesia (4%). Two weeks after inoculation, the mice, now weighing about 30 g and bearing tumors of 5–11 mm^3 in diameter, were used for *in vivo* imaging studies on a fluorescence scanner (IVIS, PerkinElmer).

Compound **5_Cy5** (80.0 μg, 72.7 nmol) was dissolved in DMSO (36.0 μL). An aliquot of this solution (5 μL) was added to 0.9% saline

(495 μL) to obtain a solution of **5_Cy5** (20 μM), which was injected (100 μL, 2 nmol/mice) intravenously (n = 2) or subcutaneously (n = 2) under isoflurane anesthesia (4%). As a control for the comparative study, the dye **Cy5**-OH (40 μg, 77 nmol) was formulated to obtain a 20 μM solution for intravenous (100 μL, 2 nmol/mice, n = 2) or subcutaneous injection (n = 1) under isoflurane anesthesia (4%). Fluorescence imaging was performed using a Cy5-filter (excitation: 640 nm, emission: 680 nm) at an exposure time of 0.2 or 0.5 s and a binning factor of 2 or 4 after 1, 3, 5 and 24 h post injection while the mice were under isoflurane anesthesia (4%) and on a heat mat (37 °C). Images were qualitatively analyzed at each period of time using the same conditions for image acquisition. After the final *in vivo* scan (at 24 h after injection of **5_Cy5** or **Cy5**-OH, respectively), the mice were euthanized under isoflurane anesthesia (4%) by cervical dislocation. Organs of interest were collected and arranged on a white background for fluorescence imaging (excitation: 640 nm, emission: 680 nm) at an exposure time of 0.75 s and a binning factor of 4. In addition, the tumors of all mice were placed in the field of view of the fluorescence scanner and image acquisition was started using an exposure time of 2 s and a binning factor of 8. The light emission from the region of interest of each tissue was quantified using Living Image® software (vers. 4.5, PerkinElmer) as radiant efficiency and values were provided as mean values ± standard deviation.

Acknowledgements

We thank German Research Council (DFG) for funding: grants DFG 1418/7-2 and DFG MA 4295/2-1. Partial funding of this project was provided by the European Union's Horizon 2020 research and innovation programme under the Marie Skłodowska-Curie grant agreement No. 872331: NoBiasFluors. We thank Mr. Manuel Geisthoff for excellent technical assistance. A part of this work has been previously published as a PhD thesis using the institutional repository and online publication system OPUS FAU which is the central electronic archiving and publication platform for all members of FAU.[10] The initial publication on OPUS FAU does not legally preclude further publication of the document in journals or monographs as well as on other repositories. Open Access funding enabled and organized by Projekt DEAL.

Conflict of Interest

The authors declare no conflict of interest.

Keywords: Anticancer · Ferrocene · Imaging · Prodrug · Reactive oxygen species

[1] a) S. Daum, V. Chekhun, I. Todor, N. Lukianova, Y. Shvets, L. Sellner, K. Putzker, J. Lewis, T. Zenz, I. Graaf, G. Groothuis, A. Casini, O. Zozulia, F. Hampel, A. Mokhir, *J. Med. Chem.* **2015**, *58*, 2015–2024; b) H. Hagen, P. Marzenell, E. Jentzsch, F. Wenz, M. R. Veldwijk, A. Mokhir, *J. Med. Chem.* **2012**, *55*, 924–934; c) P. Marzenell, H. Hagen, L. Sellner, T. Zenz, R. Grinyte, V. Pavlov, S. Daum, A. Mokhir, *J. Med. Chem.* **2013**, *56*, 6935–6944.

[2] a) F. Antunes, R. Cadenas, *FEBS Lett.* **2000**, *475*, 121–126; b) J. R. Stone, *Archiv. Biochem. Biophys.* **2004**, *422*, 119–124.

[3] a) H. Xu, M. Schikora, M. Sisa, S. Daum, I. Klemt, C. Janko, C. Alexiou, G. Bila, R. Bilyy, W. Gong, M. Schmitt, L. Sellner, A. Mokhir, *Angew. Chem. Int. Ed.* **2021**, *60*, 11158–11162; *Angew. Chem.* **2021**, *133*, 11258–11262; b) V. Reshetnikov, S. Daum, C. Janko, W. Karawacka, R. Tietze, C. Alexiou, S. Paryzhak, T. Dumych, R. Bilyy, P. Tripal, B. Schmid, R. Palmisano, A. Mokhir, *Angew. Chem.* **2018**, *130*, 12119–12122; *Angew. Chem. Int. Ed.* **2018**, *57*, 11943–11946; c) S. Daum, V. Reshetnikov, M. Sisa, T. Dumych, M. D. Lootsik, R. Bilyy, E. Bila, C. Janko, A. Alexiou, M. Herrmann, L. Sellner, A. Mokhir, *Angew. Chem.* **2017**, *129*, 15751–15755; *Angew. Chem. Int. Ed.* **2017**, *56*, 15545–15549.

[4] S. Daum, S. Babiy, H. Konovalova, W. Hofer, A. Shtemenko, N. Shtemenko, C. Janko, C. Alexiou, A. Mokhir, *J. Inorg. Biochem.* **2018**, *178*, 9–17.

[5] S. Daum, J. Toms, V. Reshetnikov, H. G. Özkan, F. Hampel, S. Maschauer, A. Hakimioun, F. Beierlein, L. Sellner, M. Schmitt, O. Prante, A. Mokhir, *Bioconjugate Chem.* **2019**, *30*, 1077–1086.

[6] S. Maschauer, R. Haubner, T. Kuwert, O. Prante, *Mol. Pharm.* **2014**, *11*, 505–515.

[7] J. Toms, V. Reshetnikov, S. Maschauer, A. Mokhir, O. Prante, *J. Labelled Comp. Radiopharm.* **2018**, *61*, 1081–1088.

[8] V. Reshetnikov, H. G. Özkan, S. Daum, C. Janko, C. Alexiou, C. Sauer, M. R. Heinrich, A. Mokhir, *Molecules* **2020**, 25, 2545.

[9] The usual abbreviation for photoinduced electron transfer is "PET". We use in this paper the abbreviation "PE", since "PET" was already previously reserved for positron emission tomography.

[10] J. Toms. Development of 18F-labeled radiotracers for imaging of reactive oxygen species and the fibroblast activation protein in tumors by positron emission tomography, PhD thesis, **2021**, Friedrich-Alexander-Universität Erlangen-Nürnberg (FAU), urn:nbn:de:bvb:29-opus4–170012.

Manuscript received: September 24, 2021
Revised manuscript received: November 9, 2021
Accepted manuscript online: November 10, 2021